208Pb(16O, 15O)209Pb Reaction

Authors
Becchetti, F D
Harvey, B G
Kovar, D
et al.

Publication Date
1975-02-01

Published in the Physical Review C,
Vol. 12, No. 3, 894 - 900
(September 1975)

$^{208}Pb(^{16}O, ^{15}O)^{209}Pb$ REACTION

F. D. Becchetti, B. G. Harvey, D. Kovar,
J. Mahoney, C. Maguire, and D. K. Scott

February 24, 1975

Prepared for the U. S. Energy Research and
Development Administration under Contract W-7405-ENG-48

DISCLAIMER

$^{208}Pb(^{16}O, ^{15}O)^{209}Pb$ reaction*

F. D. Becchetti
Cyclotron Laboratory, Department of Physics, The University of Michigan, Ann Arbor, Michigan 48104 and Lawrence Berkeley Laboratory, Berkeley, California 94720

B. G. Harvey, D. Kovar,† J. Mahoney, C. Maguire, and D. K. Scott
Lawrence Berkeley Laboratory, Berkeley, California 94720
(Received 24 February 1975)

The neutron levels in ^{209}Pb have been studied with the $^{208}Pb(^{16}O,^{15}O)$ reaction at a bombarding energy of 139 MeV. Spectroscopic factors (S) have been deduced using a finite-range distorted-wave Born approximation (DWBA) with recoil. The $2g_{9/2}$, $1i_{11/2}$, $2g_{7/2}$, and $3d_{3/2}$ levels are found to have $S \gtrsim 0.9$ while $S \approx 0.7$ for the $1j_{15/2}$ level at 1.4 MeV excitation. Evidence is found for other $1j_{15/2}$ fragments being at 3.05 MeV and ~ 3.8 MeV with $S \approx 0.08$ and 0.26, respectively, which would place the centroid of the $1j_{15/2}$ level at $E_x \approx 2.2$ MeV. DWBA predicts a shift in the maxima of the angular distributions as a function of Q value which is not observed experimentally. A comparison with the proton transfer reaction $^{208}Pb(^{16}O,^{15}N)^{209}Bi$ has been used to deduce the geometrical parameters of a neutron shell-model potential appropriate for nuclei with $A \gtrsim 200$. The parameters of this Woods-Saxon potential are: $V_R = -50.5$ MeV, $r_R = 1.19$ fm, $a_R = 0.75$ fm, $V_{so} = -5.5$ MeV, $r_{so} = 1.01$ fm, and $a_{so} = 0.75$ fm.

[NUCLEAR REACTIONS $^{208}Pb(^{16}O, ^{15}O)$, $E = 139$ MeV; measured $\sigma(E_f, \theta)$; DWBA analysis; ^{209}Pb deduced spectroscopic factors, nuclear shell-model potential. Magnetic spectrometer; resolution 180 to 240 keV.]

I. INTRODUCTION

Previous studies of the neutron levels in ^{209}Pb via stripping reactions such as (d,p),[1-3] (t,d),[4] and $(\alpha, {}^3He)$[5] indicate that some of the expected single particle strength, particularly for the $1j_{15/2}$ level, is fragmented.[2-5] Analysis of data from the $^{208}Pb(^{16}O, ^{15}O)$ reaction can provide additional, complimentary information concerning the high spin levels in ^{209}Pb, since the $(^{16}O, ^{15}O)$ reaction favors much higher l transfers than most light-ion reactions. Also, from such an analysis one may learn about the form of the neutron shell-model potential in heavy nuclei, the relative proton and neutron density distributions in these nuclei, and the single-particle levels for $A \gtrsim 200$, especially in the region of "superheavy" nuclei ($A \approx 300$).

II. EXPERIMENTAL TECHNIQUES

The experiment was performed at the Lawrence Berkeley Laboratory 88-inch cyclotron with a 139 MeV ^{16}O (4^+) beam [in experiments at 104 MeV, the $(^{16}O, ^{15}O)$ cross sections were at least an order of magnitude smaller than those at 139 MeV]. The targets consisted of 100–150 $\mu g/cm^2$ enriched ^{208}Pb evaporated onto carbon backings, 20–30 $\mu g/cm^2$ thick. The reaction products were detected and identified with a position-sensitive proportional counter[6] in the focal plane of an energy-loss magnetic spectrometer. The energy resolution was 180–240 keV full width at half-maximum FWHM.

Differential cross sections were determined by comparison with forward angle elastic scattering, which was assumed to be equal to Rutherford scattering. Charge state ratios were determined using the elastic scattering of ^{16}O. The carbon backing on the target was placed facing the entrance to the spectrometer so as to assure a constant charge state distribution for reaction products independent of carbon buildup on the target. Angular distributions were measured near the grazing angle expected for direct single-neutron transfer. The absolute cross sections are estimated to be accurate to ±15%.

An $^{15}O^{8+}$ spectrum is shown in Fig. 1 (note log scale). Groups which were identified at three or more angles are indicated. The $4s_{1/2}$ level (E_x = 2.05 MeV) was not observed at the particular angle shown but was seen at other angles. Groups which can be attributed to trace (<2%) amounts of ^{206}Pb and ^{207}Pb in the target are not labeled. Kinematic considerations exclude particles due to light contaminants. The groups seen in Fig. 1 may be due to states in ^{209}Pb, ^{15}O, or both.

Only three levels[1-4] in ^{209}Pb are populated with appreciable strength: $2g_{9/2}$ (ground state), $1i_{11/2}$ ($E_x = 0.8$ MeV), and $1j_{15/2}$ ($E_x = 1.45$ MeV). We note also the j dependence which favors $j_>(\equiv l + \frac{1}{2})$ states

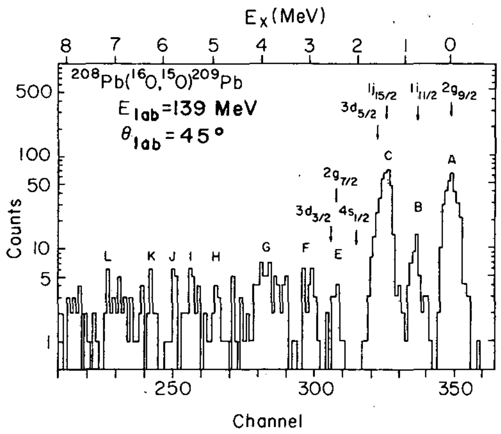

FIG. 1. An $^{208}Pb(^{16}O, ^{15}O)$ spectrum taken near the grazing angle. The position of states in ^{209}Pb of known spin and parity are indicated by arrows, while groups identified in this experiment are labeled (A-L).

relative to $j_<$ ($\equiv l - \frac{1}{2}$) states, e.g., $1j_{15/2}$ compared to $1i_{11/2}$. This j selectivity is well known for the ($^{16}O, ^{15}N$) reaction.[7,8] An analysis of the peak shape of the group at $E_x = 1.45$ MeV indicates that the known $3d_{5/2}$ level at $E_x = 1.57$ MeV contributes $\lesssim 10\%$ to the observed peak. The first excited states in ^{15}O are at $E_x > 5.18$ MeV,[9] therefore, groups observed above ~5 MeV excitation could be due to projectile excitation. Groups due to such excitation should be much broader (~300–400 keV) than the other groups due to Doppler broadening by γ decay in flight.[10] Groups labeled I and L in Fig. 1 are likely candidates for projectile excitation as there are levels in ^{15}O near these energies.[9] The measured excitation energies and partial integrated cross sections ($\theta_{c.m.} \approx 35°$ to $65°$) are given in Table I.

Angular distributions are shown in Fig. 2. They are mostly bell-shaped curves typical of single nu-

TABLE I. Levels Observed in ^{209}Pb.

	This work ($^{16}O, ^{15}O$) 139 MeV				Other work (d,p) 12 MeV [a]		(d,p) 20 MeV [b]		(t,d) 20 MeV [c]	
Group [d]	E_x [e] (MeV)	Intg. σ [f] (mb)	nlj [g]	S [h]	E_x (MeV)	S	E_x (MeV)	S	E_x (MeV)	S
A	g.s.	1.35 (10)	$2g_{9/2}$	0.90	g.s.	0.78	g.s.	0.83(0.92)	g.s.	0.93
B	0.80	0.163(15)	$1i_{11/2}$	0.90	0.778	0.96	0.779	0.86(1.14)	0.781	1.05
C	1.45	1.67 (10)	$1j_{15/2}$	0.71 [i]	1.422	0.53	1.424	0.58(0.77)	1.428	0.60
			$3d_{5/2}$		1.565	0.88	1.565	0.98(0.89)	1.573	1.02
D	2.05	0.014 (7)	$4s_{1/2}$	(4.1) [j]	2.031	0.88	2.033	0.98(0.85)	2.039	1.00
E	2.49	0.121(12)	$2g_{7/2}$	(1.7) [j]	2.492	0.78	2.493	1.05(0.95)	2.496	1.05
			$3d_{3/2}$		2.537	0.88	2.537	1.07(0.99)	2.542	0.96
F	3.05	0.118(12)	($1j_{15/2}$)	0.08 [j]			3.052	0.070		
G	3.5–4.1 [k]	0.306(30) [k]	($1j_{15/2}$)	0.26 [j]			3.556	0.032		
							3.904	0.032		
H	5.00	···								
I	5.52 [l]	0.116(12) [l]			(See references for additional levels)					
J	5.88	···								
K	6.32	···								
L	7.00 [l]	0.095(10) [l]								

[a] Reference 2. E_x energies ±5 keV. (Not all observed levels are listed.)
[b] Reference 3. E_x energies ±5 keV. (Not all observed levels are listed.) The S values in parentheses are from an analysis using a deuteron breakup potential.
[c] Reference 4. E_x energies ±5 keV. (Not all observed levels are listed.)
[d] See Fig. 1.
[e] Excitation energy in ^{209}Pb and/or ^{15}O (±50 keV).
[f] Partial integrated cross sections, $\theta = 35°$ to $65°$ (c.m.). Errors in last digits are given in parentheses.
[g] Known spin of levels in ^{209}Pb (Refs. 2–4). Values in parentheses are assumed spins (see text).
[h] Spectroscopic factor for state in ^{209}Pb with $S = 1.9$ for ^{15}O g.s. (Ref. 9). Optical parameters (Ref. 11): $V = -30$ MeV, $W = -15$ MeV, $R = 1.31(A_1^{1/3} + A_2^{1/3})$ fm, $a = 0.45$ fm; bound state $n + ^{15}O$: $V_R = -56$ MeV, $R_R = 1.20A^{1/3}$ fm, $a_R = 0.65$ fm with $V_{so} = 0$; bound state $n + ^{208}Pb$: $R_R = 1.19A^{1/3}$ fm, $a_R = 0.75$ fm, $V_{so} = -5.5$ MeV, $R_{so} = 1.01A^{1/3}$ fm, $a_{so} = 0.75$ fm, and V adjusted to fit binding energy ($V_R \approx -50.5$ MeV).
[i] Corrected for small contribution ($\lesssim 10\%$) from unresolved $3d_{5/2}$ level.
[j] Approximate since fit to data is poor (see Fig. 2). The value quoted for the $2g_{7/2}$ level contains a small correction for the unresolved $3d_{3/2}$ level.
[k] Includes several states (see Fig. 1).
[l] Most likely due to transfer to excited state of ^{15}O (see text).

cleon transfers in heavy nuclei.[8,11,12] The only exceptions are the $4s_{1/2}$ level ($E_x = 2.05$ MeV) and perhaps the groups I and L ($E_x = 5.52$ and 7.00 MeV, respectively). As noted above, groups I and L are probably due to projectile excitation. We discuss separately the apparent anomalous angular distribution to the $4s_{1/2}$ level in Sec. III E.

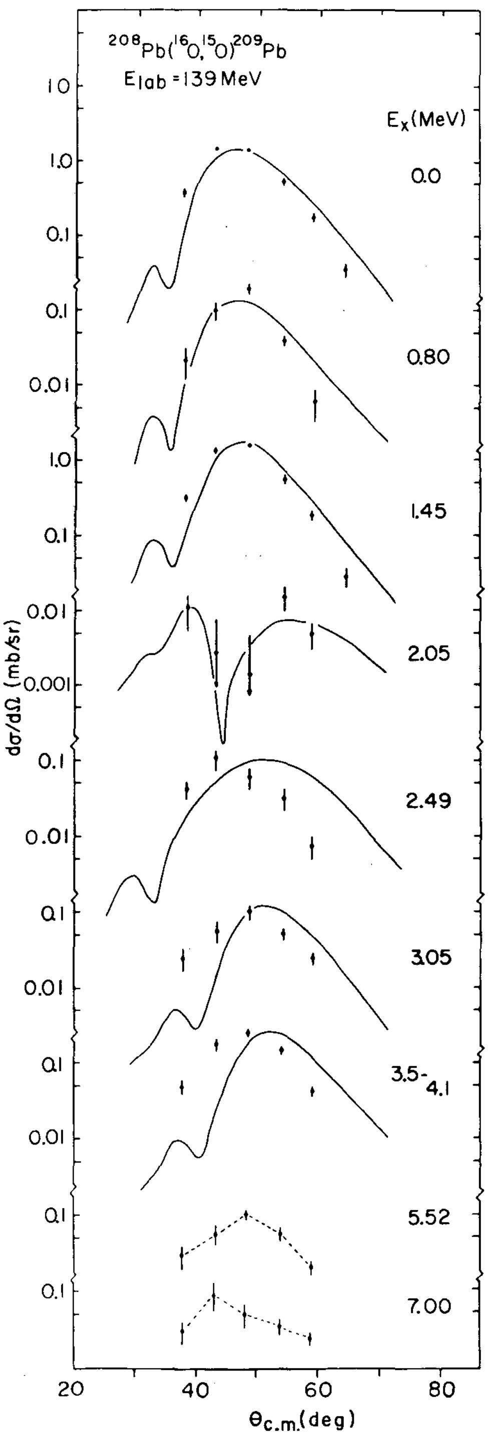

FIG. 2. ^{208}Pb(^{16}O, ^{15}O)^{209}Pb angular distributions. The solid curves are finite-range DWBA calculations. The dashed curves are only to guide the eye.

Except for the $4s_{1/2}$ level, the angular distributions do not permit direct l assignments. The systematics to the known levels indicate, however, that high spin ($l > 4$) $j_>$ states would preferentially be populated, certainly at high excitation energies. Thus the groups observed between $E_x = 2.8$ and 5 MeV are probably such levels.

III. ANALYSIS

The experimental results have been interpreted utilizing finite-range distorted-wave Born approximation (DWBA).[13] The selection rules are the same as those for (^{16}O, ^{15}N) if the transferred nucleon is assumed to be in a $1p_{1/2}$ orbital in the projectile. Thus the j dependence exhibited[7] in (^{16}O, ^{15}N) is also present in (^{16}O, ^{15}N), as can be seen in Fig. 1.

A. Determination of the neutron shell-model potential

It is known from light-ion reactions leading to ^{209}Pb that the $2g_{9/2}$, $1i_{11/2}$, $3d_{5/2}$, $4s_{1/2}$, $2g_{7/2}$, and $3d_{3/2}$ levels are reasonably pure shell-model states[1-5] ($S \approx 1$). We have used this information to determine a suitable neutron shell-model potential for ^{209}Pb. An analysis of ^{208}Pb(^{16}O, ^{15}N)^{209}Bi at the same bombarding energy has also been performed and indicates that full finite-range DWBA reproduces the measured absolute cross sections to $\leq 20\%$ if one uses potentials known to yield proton distributions consistent with measurements of the nuclear charge distributions. Although there are still questions concerning certain aspects of heavy-ion reactions, extensive analyses indicate that a proper DWBA treatment gives a good representation of the total transfer strength to single-particle states in heavy, spherical nuclei.[11,12] Furthermore, the simultaneous analysis of (^{16}O, ^{15}O) and (^{16}O, ^{15}N) reactions should provide resonably model-independent information on the target neutron wave functions relative to the proton wave functions as the projectiles are "mirror" nuclei. Thus similar projectile wave functions and optical potentials can be used in the analysis of the two reactions. In our analysis of (^{16}O, ^{15}O) we therefore used optical model and projectile bound-state parameters similar to those used in analysis of (^{16}O, ^{15}N) on ^{208}Pb and varied only the parameters determining the potential binding the neutrons in ^{209}Pb. The sensitivity of the DWBA calculations to variations of the optical model and bound-state parameters is similar to that found by other groups.[11,12,14] We required that the binding potential, when used in DWBA, reproduce relative to

$(^{16}O,^{15}N)$ the observed $(^{16}O,^{15}O)$ cross sections to single-particle states and, if possible, give the observed level position.

Among the target neutron potentials tried, a modified form of the Zaidi-Darmodjo potential[15] yielded the most acceptable results. The modification consisted of adopting spin-orbit parameters deduced from study of neutron-nucleus elastic scattering.[16] This potential has $R_{so} < R_R$ and yields a better fit to the observed single-particle energies in ^{209}Pb compared to the unmodified potential.

The neutron bound-state potential deduced from our analysis has the following parameters (Woods-Saxon well):

$$V_R = -50.5 \text{ MeV}, \quad R_R = 1.19A^{1/3} \text{ fm}, \quad a_R = 0.75 \text{ fm},$$
$$V_{so} = -5.5 \text{ MeV}, \quad R_{so} = 1.01A^{1/3} \text{ fm}, \quad a_{so} = 0.75 \text{ fm}. \tag{1}$$

The potential (1) which we will denote as MZD (modified Zaidi-Darmodjo) is similar to those used to fit neutron-nucleus scattering.[16] The MZD potential, however, is different from those determined by fitting energy levels alone ($r_R = 1.25$ to 1.40 fm). The latter potentials, such as those determined by Batty and Greenlees[17] or Rost,[18] give neutron wave functions which, when used in DWBA, overestimate the $(^{16}O,^{15}O)$ cross sections by factors of 2 to 3. The energies of single-particle levels in ^{209}Pb predicted using the MZD potential, except for the $1j_{15/2}$ level which is fragmented (see next section), are reproduced to 400 keV or less. The calculated position of the $1j_{15/2}$ level is incorrect (by 1.4 MeV) even if we take the $1j_{15/2}$ centroid energy, however. The problems of fitting, simultaneously, neutron level positions and transfer data have been noted and discussed by several authors.[19,20] It is concluded that the potential binding nucleons in heavy nuclei is more complicated than the simple shell-model potential used here.

The implications of potential (1) regarding neutrons in nuclei $A > 200$ are discussed in more detail in Sec. IV.

B. $1j_{15/2}$ level

Using the parameters which give $S \approx 1$ for the strong transitions to known single-particle states ($2g_{9/2}$ and $1i_{11/2}$) we obtain $S = 0.71$ for the $1j_{15/2}$ level at $E_x = 1.45$ MeV. There are two primary candidates for the missing $1j_{15/2}$ fragments, namely, the (unresolved) groups F and G (see Fig. 1) at $E_x = 3.05$ and 3.5 to 4.1 MeV. High spin levels ($l > 6$) at these energies are also observed[3,5] in $^{208}Pb(d,p)$ and $^{208}Pb(\alpha,{}^3He)$. Their observation in $(^{16}O,^{15}O)$ indicates that they are probably $1j_{15/2}$ ($j_>$) fragments. Assuming $nlj = 1j_{15/2}$ for these groups, we obtain $S = 0.08$ and 0.26, respectively, for groups F and G; the latter being a combination of unresolved levels. Inclusion of these groups as $1j_{15/2}$ states exhausts the single-particle strength ($S \rightarrow 1$) and, more importantly, places the centroid for the $1j_{15/2}$ level at $E_x \approx 2.2$ MeV. This result is to be compared with the value $E_x = 1.78$ MeV determined from a study[3] of $^{208}Pb(d,p)$.

The observed fragmentation of the $1j_{15/2}$ strength agrees very well with predictions of the weak coupling model made by Bes and Broglia.[21] They predict the following energies and spectroscopic factors for the main $1j_{15/2}$ fragments[3,21]: $E_x = 1.41$ MeV, $S = 0.65$; $E_x = 3.22$ MeV, $S = 0.17$; and $E_x = 3.47$ MeV, $S = 0.30$, whereas we observe (Table I) $E_x = 1.45$ MeV, $S = 0.71$; $E_x = 3.05$, $S = 0.08$; and $E_x = 3.5$–4.1 MeV, $S = 0.26$.

C. Other known levels

Spectroscopic factors and the corresponding fits to the $(^{16}O,^{15}O)$ data for all the known single-particle levels in ^{209}Pb are given in Table I and Fig. 2. The preferred l transfer for $^{208}Pb(^{16}O,^{15}O)$ is $\gtrsim 10$. Thus transfers to all but the $2g_{9/2}$, $1i_{11/2}$, and $1j_{15/2}$ states are badly momentum mismatched and the cross sections are therefore small. Also, the DWBA fits are poor and thus the spectroscopic factors are not well determined for $E_x > 2$ MeV. The values deduced from the fits shown in Fig. 2 are listed in Table I. One can obtain $S \sim 1$, however, if other fitting criteria are used.

D. Levels $E_x > 5$ MeV

As noted previously, levels seen above $E_x = 5$ MeV may be due to projectile excitation and/or excitation of ^{209}Pb. As seen in Fig. 1, however, there are no groups populated with much intensity at energies above 5 MeV. Our calculations indicate that certain high spin $j_>$ states ($3f_{7/2}$, $1k_{17/2}$, $2h_{11/2}$, etc.) would have been seen if their spectroscopic factors were on the order of unity. The observed intensities ($\lesssim 0.1$ μb/sr) for levels between $E_x = 5$ and 10 MeV correspond to $S \lesssim 0.1$ for any high spin $j_>$ single-particle fragments in this energy region. This observation is consistent with results from recent (d,p) and $(\alpha,{}^3He)$ experiments.[3,5] The former experiment indicates that there is no appreciable single-particle strength between $E_x = 3$ and 6 MeV in ^{209}Pb. The absence of pure single-particle states several MeV beyond the known $3d_{3/2}$ and $2g_{7/2}$ levels is significant in that this energy region spans the gap associated with the possible shell closure at $N = 184$ (see Sec. IV).

E. Anomalous angular distribution to the $4s_{1/2}$ level

As noted above, the observed $(^{16}O,^{15}O)$ angular distributions are mostly bell shaped (Fig. 2). A notable exception is that for the $4s_{1/2}$ level at $E_x = 2.05$ MeV. The transition to this level is unique in that only a single l transfer, $L=1$, is allowed, whereas two l transfers are normally permitted (if recoil is included). In contrast with the other data, the cross section to the $4s_{1/2}$ level has a minimum near the grazing angle ($\theta \sim 45°$). This feature is reproduced by full finite-range DWBA however (see Fig. 2).

The distinct shape of the angular distribution for the $4s_{1/2}$ level and the unique feature of a single allowed l transfer permit one to investigate certain effects. The origin of the minimum in the $4s_{1/2}$ angular distribution at the grazing angle, for example, can be related to the magnetic substate (M) population. Since $L=1$ only $M=-1$, 0, and $+1$ can contribute, i.e., $|M|=0$ and 1. Classical expressions for $|M|=0$ and 1 substate populations have been derived[22] and indicate that for transfers where the Q match is poor, as here for the $4s_{1/2}$ level, the $|M|=0$ and 1 populations should be comparable. Thus, one may observe appreciable contributions from all M states. In contrast, transitions where Q matching is good, one $|M|$ value dominates and produces a bell-shaped angular distribution.[22]

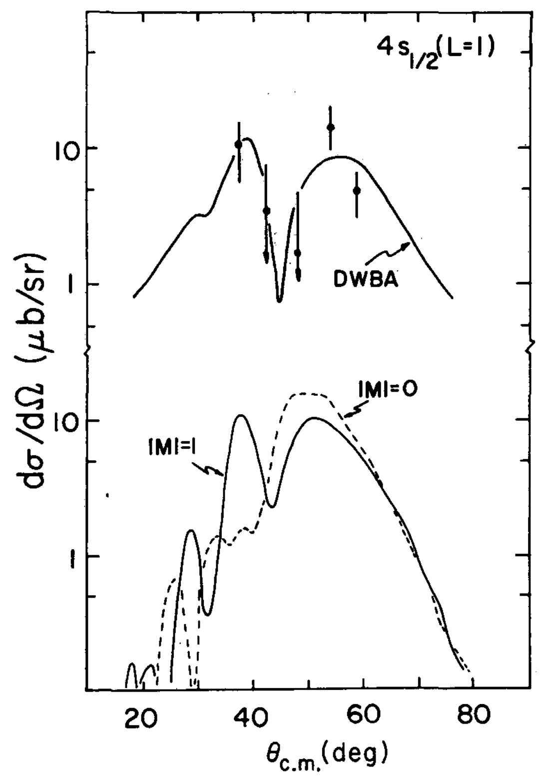

FIG. 3. Top: The observed angular distributions to the $4s_{1/2}$ level in ^{209}Pb compared with a finite-range DWBA calculation ($L=1$). Bottom: Decomposition of a DWBA calculation (excluding recoil) for the $4s_{1/2}$ level into the magnetic substate population. (The cross section scale for the no-recoil DWBA calculations has been arbitrarily renormalized.)

We illustrate these features in Fig. 3 where we decompose a DWBA calculation (no recoil) into different M-state partial cross sections. The z axis is taken along the beam axis (notation of Ref. 23). The observed angular distribution appears to show structure due to the $|M|=1$ component of the cross section. Some differences between calculations with and without recoil are indicated although this may be due to the numerical procedures used in the programs. Detailed study of transitions involving unique M-state populations may hopefully elucidate some features of the heavy-ion transfer mechanism.

F. No-recoil DWBA calculations

In addition to calculations with DWBA including recoil we have also, for comparison, performed no-recoil DWBA calculations[23] using the same parameters. Surprisingly, perhaps, the cross sections to the $j_>$ states ($2g_{9/2}$, $1j_{15/2}$, and also $4s_{1/2}$) are predicted to within about a factor of 3. As expected, however, the cross sections to the $j_<$ states ($1i_{11/2}$, $2g_{7/2}$, etc.) are grossly (by more than a factor of 100) underestimated. This discrepancy is much greater than that observed[11] for ^{208}Pb(^{16}O,^{15}N) but is of the order expected from the recoil effects predicted by Buttle and Goldfarb.[24]

G. Shifts in angular distributions

It has been observed that heavy-ion stripping reactions such as (^{16}O,^{15}N) and (^{12}C,^{11}B) exhibit a peculiar behavior: The peak in the measured angular distributions shifts little, if at all, with Q value, whereas DWBA and classical models both predict large shifts.[8,11,12,25] It has been suggested that this feature may be related to transfer of charge.[26] Our (^{16}O,^{15}O) data and other recent neutron stripping data[12] show effects similar to those observed for proton transfers: DWBA predicts a much larger shift in peak position than is observed experimentally (see Fig. 2). The observation of these features in both proton and neutron stripping reactions excludes effects related to charge transfer as an explanation of this phenomenon. It appears, rather, that the simple optical-model description of the ion-ion interaction is not entirely adequate in describing projectile orbits for transfer processes between heavy ions.

IV. NEUTRONS IN NUCLEI, $A \gtrsim 200$

Neutron potentials such as (1) have important implications concerning two problems of current interest: the neutron distribution in ^{208}Pb, i.e.,

$A \approx 200$ and the ordering of neutron levels in superheavy nuclei ($A \approx 300$).

A. Neutron distribution in ^{208}Pb

Since a transfer reaction, such as $^{208}Pb(^{16}O, ^{15}O)$-^{209}Pb, is a probe of neutron wave functions, potentials such as MZD which are determined by fitting transfer data should represent the average potential appropriate to the valence neutrons in nuclei, $A \approx 200$. We have used the MZD potential to generate the spatial distribution of the N-Z excess neutrons in ^{208}Pb. The rms radius of this distribution, $\langle r_{exc}^2\rangle^{1/2}$, is 5.89 fm. The rms radius of the total neutron distribution, $\langle r_n^2\rangle^{1/2}$, in ^{208}Pb has then been calculated in two different ways: First we have used $\langle r_{exc}^2\rangle^{1/2}$ determined from the MZD potential and then assumed that the $N=Z$ core neutrons have the same rms radius as the measured proton distribution[27]($\langle r_p^2\rangle^{1/2} = 5.43$ fm). Secondly, we have used the MZD potential to calculate all neutron wave functions, i.e., including those of the $N=Z$ core neutrons. The values of $\langle r_n^2\rangle^{1/2}$ and $\langle r_n^2\rangle^{1/2} - \langle r_p^2\rangle^{1/2}$ deduced with the two methods are consistent with $\langle r_n^2\rangle^{1/2} - \langle r_p^2\rangle^{1/2} \approx 0.1 \pm 0.1$ fm in ^{208}Pb.

The results of our calculations may be compared with other calculated or "measured" values of $\langle r_n^2\rangle^{1/2}$ and $\langle r_n^2\rangle^{1/2} - \langle r_p^2\rangle^{1/2}$.[28-32] The values of $\langle r_n^2\rangle^{1/2}$ calculated with potentials determined by fitting neutron energy levels[17-19] are ~0.5 fm larger than that deduced with the MZD potential. Also, neutron radii determined from analysis of α-nucleus[28] or p-nucleus[29] elastic scattering using folding models are about 0.1 to 0.3 fm larger. The neutron radii determined from analyses of Coulomb displacement energies,[30] pion reaction cross sections,[31] and (d,t) and (p,d) reactions[20] are comparable to those deduced here, however. Analysis of nucleon bremsstrahlung[32] gives $\langle r_n^2\rangle^{1/2}$ less than $\langle r_p^2\rangle^{1/2}$ by ~0.15 fm. It should be noted that the present analysis of neutron and proton stripping from ^{16}O and the analysis[31] of π^+ and π^- reaction cross sections should be especially sensitive to differences in the neutron and proton distributions and both of these analyses indicate $\langle r_n^2\rangle^{1/2} \approx \langle r_p^2\rangle^{1/2}$ for $A \approx 200$.

Recent experiments[33] which indicate a neutron "halo" in ^{208}Pb are not necessarily inconsistent with $\langle r_n^2\rangle^{1/2} \approx \langle r_p^2\rangle^{1/2}$ since the nuclear Coulomb potential necessarily dampens the proton wave functions at large radii and produces a neutron halo. The halo factor is defined as the ratio of the neutron and proton distributions normalized by N/Z, i.e., $(\rho_N/\rho_P)/(N/Z)$. The experimental value (2.34 ± 0.50) is deduced from analysis[33] of antiproton absorption in Pb. We have compared this with values calculated from neutron densities determined with the MZD potential (1) and the Batty-Greenlees neutron potential.[17] The MZD potential yields the observed neutron halo at ~9.5 fm, while for the BG potential and similar neutron potentials this occurs at ~7.5 fm. The former radius corresponds to a nucleon density a few percent that of the central density while the latter about 30%. It is believed that antiproton absorption, however, occurs mainly in the periphery, i.e., low density regions of nuclei. If this is true, then the MZD potential is a more appropriate neutron potential.

Thus we conclude that analyses of Coulomb displacement energies, π-meson, and antiproton absorption as well as nucleon transfer reactions are consistent with ^{208}Pb having neutron and proton distributions with similar rms radii but this does not exclude a neutron "halo" in the periphery.

B. Neutron levels $A \approx 300$

The ordering of neutron levels in nuclei $A \approx 300$ predicted by the MZD potential has been calculated and is discussed elsewhere.[34] A large energy gap (>3 MeV) is predicted at neutron number $N = 184$, with smaller gaps at $N = 148$ and 210. The prediction of a wide energy gap at $N = 184$ is consistent with the lack of apparent single-particle strength above $E_x = 3$ MeV in ^{209}Pb as observed in $(^{16}O, ^{15}O)$ and other neutron transfer reactions (see Sec. III D). The level sequence predicted by the MZD potential differs from those of many other models (see review in Ref. 35) although most simple potentials predict the gap at $N = 184$.

V. CONCLUSIONS

The analysis of data from the reaction ^{208}Pb-$(^{16}O, ^{15}O)^{209}Pb$ at $E_{1ab} = 139$ MeV indicates the following:

(1) About 70% of the $1j_{15/2}$ single-particle strength is at $E_x \approx 1.5$ MeV, while other fragments are likely at $E_x \approx 3.0$ MeV (~8%) and between $E_x = 3.5$ and 4.1 MeV (~26%).

(2) The magnitude of the $(^{16}O, ^{15}O)$ transfer cross sections relative to $(^{16}O, ^{15}N)$ can be reproduced with finite-range DWBA if a modified form of the Zaidi-Darmodjo potential is used to generate the neutron wave functions in ^{209}Pb. This potential produces a neutron distribution in Pb having an rms radius similar to that of the known proton distribution, but this does not exclude the presence of a neutron halo in the periphery of Pb.

(3) As also observed for proton stripping, the $(^{16}O, ^{15}O)$ angular distributions as a function of Q value are not fitted well with DWBA.

ACKNOWLEDGMENTS

We thank R. DeVries and A. Baltz for their assistance with the DWBA calculations, and the cyclotron crew at Lawrence Berkeley Laboratory for their help during the experiment. We also thank M. Zisman, H. Homeyer, and W. von Oertzen for their help in taking data.

---

*Work supported in part by U.S. Atomic Energy Commission contracts Nos. AEC AT(11-1)-2167 and W-7405-ENG-48.

†Present address: Physics Division, Argonne National Laboratory, Argonne, Illinois 60439.

[1]G. Muehllehner, A. S. Poltorak, W. C. Parkinson, and R. H. Bassel, Phys. Rev. 159, 1039 (1967).

[2]C. Ellegaard, J. Kantele, and P. Vedelsby, Nucl. Phys. A129, 113 (1969).

[3]D. G. Kovar, N. Stein, and C. K. Bockelman, Nucl. Phys. A231, 266 (1974).

[4]G. J. Igo, P. D. Barnes, E. R. Flynn, and D. D. Armstrong, Phys. Rev. 177, 1831 (1969).

[5]R. S. Tickle and W. C. Parkinson, Cyclotron Laboratory, The University of Michigan, Annual Report, 1972, (unpublished), p. 52; R. Tickle and W. S. Gray, Bull. Am. Phys. Soc. 19, 1020 (1974).

[6]B. G. Harvey *et al.*, Nucl. Instrum. Methods 104, 21 (1972).

[7]D. G. Kovar, F. D. Becchetti, B. G. Harvey, F. G. Pühlhofer, J. Mahoney, D. W. Miller, and M. S. Zisman, Phys. Rev. Lett. 29, 1023 (1972).

[8]H. J. Körner, G. C. Morrison, L. R. Greenwood, and R. H. Siemssen, Phys. Rev. C 7, 107 (1973); P. R. Christensen, V. I. Manko, F. D. Becchetti, and R. J. Nickles, Nucl. Phys. A207, 33 (1973).

[9]F. Ajzenberg-Selove, Nucl. Phys. A152, 127 (1970), and references cited therein.

[10]M. S. Zisman, F. D. Becchetti, B. G. Harvey, D. G. Kovar, J. Mahoney, and J. D. Sherman, Phys. Rev. C 8, 1866 (1973).

[11]D. G. Kovar, B. G. Harvey, F. D. Becchetti, J. Mahoney, D. L. Hendrie, H. Homeyer, W. von Oertzen, and M. A. Nagarajan, Phys. Rev. Lett. 30, 1075 (1973).

[12]J. L. C. Ford, Jr., K. S. Toth, G. R. Satchler, D. C. Hensley, L. W. Owen, R. M. DeVries, R. M. Gaedke, P. J. Riley, and S. T. Thorton, Phys. Rev. C 10, 1429 (1974).

[13]R. M. DeVries, Phys. Rev. C 8, 951 (1973); program LOLA, R. M. DeVries, University of Washington (unpublished); A. Baltz (private communication).

[14]A. R. Barnett, W. R. Phillips, P. J. A. Buttle, and L. J. B. Goldfarb, Nucl. Phys. A176, 321 (1971).

[15]S. A. A. Zaidi and S. Darmodjo, Phys. Rev. Lett. 19, 1446 (1967).

[16]F. Becchetti and G. W. Greenlees, Phys. Rev. 182, 1190 (1969).

[17]C. J. Batty and G. W. Greenlees, Nucl. Phys. A133, 673 (1969).

[18]E. Rost, Phys. Lett. 26B, 184 (1968).

[19]C. J. Batty, Phys. Lett. 31B, 496 (1970).

[20]H. J. Körner and J. P. Schiffer, Phys. Rev. Lett. 27, 1457 (1971); J. P. Schiffer and H. J. Körner, Phys. Rev. C 8, 841 (1973).

[21]D. Bes and R. Broglia, Phys. Rev. C 3, 2389 (1971).

[22]C. Chasman, S. Kahana, and M. Schneider, Phys. Rev. Lett. 31, 1074 (1973); S. Kahana, P. D. Bond, and C. Chasman, Phys. Lett. 50B, 199 (1974).

[23]Program DWUCK, P. D. Kunz, University of Colorado Report No. COO-535-613, 1971 (unpublished); program RDRC, W. Tobocman (unpublished).

[24]P. J. A. Buttle and L. J. B. Goldfarb, Nucl. Phys. 78, 409 (1966); A176, 299 (1971).

[25]J. S. Larsen, J. L. C. Ford, Jr., R. M. Gaedke, K. T. Toth, J. B. Ball, and R. L. Hahn, Phys. Lett. 42B, 205 (1972); J. V. Maher, K. A. Erb, and R. W. Miller, Phys. Rev. C 7, 651 (1973).

[26]W. von Oertzen, Argonne Laboratory Report No. PHY-1973B, 1973 (unpublished), p. 675.

[27]H. L. Acker, G. Backenstoss, C. Daum, J. C. Sens, and S. A. de Witt, Nucl. Phys. 87, 1 (1966).

[28]B. Tatischeff, I. Brissaud, and L. Bimbot, Phys. Rev. C 5, 234 (1972).

[29]G. W. Greenlees, V. Hnizdo, O. Karban, J. Lowe, and W. Makofske, Phys. Rev. C 2, 1063 (1970).

[30]J. A. Nolen, Jr., and J. P. Schiffer, Annu. Rev. Nucl. Sci. 19, 471 (1969).

[31]B. W. Allardyce *et al.*, Nucl. Phys. A209, 1 (1973).

[32]R. Leonardi, Phys. Lett. 43B, 455 (1973).

[33]W. M. Bugg, G. T. Condo, E. L. Hart, H. O. Cohn, and R. D. McCulloch, Phys. Rev. Lett. 31, 475 (1973).

[34]F. Becchetti, B. G. Harvey, D. Kovar, J. Mahoney, C. Maguire, and D. K. Scott, in *Reactions Between Complex Nuclei*, edited by R. L. Robinson *et al.*, (North-Holland, Amsterdam, 1974), Vol. 1, p. 165.

[35]P. E. Nemirovskii and B. N. Vinogradov, Yad. Fiz. 14, 972 (1971) [Sov. J. Nucl. Phys. 14, 545 (1972)].

This report was done with support from the United States Energy Research and Development Administration. Any conclusions or opinions expressed in this report represent solely those of the author(s) and not necessarily those of The Regents of the University of California, the Lawrence Berkeley Laboratory or the United States Energy Research and Development Administration.